Acta Crystallographica Section F
Structural Biology and Crystallization Communications
ISSN 1744-3091

Crystallization and preliminary X-ray crystallographic studies of the oligomeric death-domain complex between PIDD and RAIDD

Hyun Ho Park and Hao Wu*

Department of Biochemistry, Weill Medical College and Graduate School of Medical Sciences of Cornell University, New York, NY 10021, USA

Correspondence e-mail: haowu@med.cornell.edu

Received 5 January 2007
Accepted 16 February 2007

Three large macromolecular complexes known as the death-inducing signaling complex (DISC), the apoptosome and the PIDDosome mediate caspase activation in apoptosis signaling pathways. The PIDDosome, which activates caspase-2, is composed of three protein components: PIDD, RAIDD and caspase-2. Within the PIDDosome, the interaction between PIDD and RAIDD is mediated by a homotypic interaction between their death domains (DDs). PIDD DD and RAIDD DD were overexpressed in *Escherichia coli* with engineered C-terminal His tags. The proteins were purified and mixed to allow complex formation. Gel-filtration and multi-angle light scattering (MALS) analyses showed that the complex is around 150 kDa in solution. The purified PIDD DD–RAIDD DD complex was crystallized at 293 K. X-ray diffraction data were collected to resolutions of 3.2 and 4.0 Å from a native and a Hg-derivative crystal, respectively. The crystals belong to space group $P6_5$, with unit-cell parameters $a = b = 138.4$, $c = 207.6$ Å.

1. Introduction

Caspases are cysteine proteases that are essential in the initiation and execution of apoptosis and inflammation (Riedl & Shi, 2004). The formation of large oligomeric protein complexes is critical for caspase activation in apoptotic and inflammatory signaling pathways (Riedl & Shi, 2004). These oligomeric protein complexes function as a platform to recruit caspases, leading to caspase dimerization and activation *via* a proximity-induced mechanism (Salvesen & Dixit, 1999). Some well known oligomeric caspase-activating complexes include the death-inducing signaling complex (DISC) for caspase-8 activation (Wajant, 2002), the apoptosome for caspase-9 activation (Zou *et al.*, 1997), the inflammasome for caspase-1 activation (Martinon *et al.*, 2002) and the PIDDosome for caspase-2 activation (Tinel & Tschopp, 2004). The death-domain superfamily, which comprises the death domain (DD), the death-effector domain (DED), the caspase-recruitment domain (CARD) and the pyrin domain (PYD), play a pivotal role in the assembly of these oligomeric protein complexes during apoptosis and inflammation (Reed *et al.*, 2004; Park, Lo *et al.*, 2007).

The PIDDosome for caspase-2 activation consists of three components: PIDD (the p53-induced protein with a death domain), RAIDD (RIP-associated Ich-1/Ced-3 homologous protein with a death domain) and caspase-2 (Tinel & Tschopp, 2004). It is assembled *via* a DD–DD interaction between PIDD and RAIDD and a CARD–CARD interaction between RAIDD and caspase-2 (Tinel & Tschopp, 2004). Recent studies have shown that in response to genotoxic stress, caspase-2 acts upstream of the mitochondrial caspase-9 pathway to induce cell death (Lassus *et al.*, 2002).

Despite the fundamental importance of the death-domain superfamily in apoptotic and inflammatory signaling pathways, no structures of any oligomeric DD superfamily complexes are currently available. As a first step toward elucidating the molecular structure of the PIDDosome and the molecular mechanism of DD–DD oligomerization, we overexpressed, purified and crystallized the PIDD DD–RAIDD DD complex. Details of the atomic structure of this complex should enable us to understand the mechanism of PIDDosome formation *via* the DD–DD interaction.

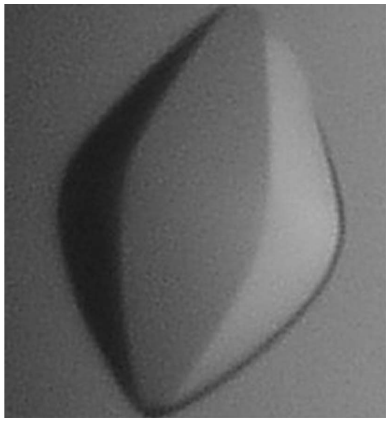

2. Materials and methods

2.1. Expression and purification

RAIDD DD was cloned and purified as described previously (Park & Wu, 2006). Purified RAIDD DD contains residues 94–199 with six C-terminal histidine residues (LEHHHHHH). The construct for PIDD DD (residues 777–883) was made as follows: the cDNA of full-length PIDD DD (isoform 3) was used as a template for PCR amplification and the plasmid vector pET-26b (Novagen) was used to add a hexahistidine tag at the carboxy-terminus of PIDD DD for affinity purification. PCR products were digested with *Nde*I and *Not*I (NEB) restriction enzymes and ligated into pET-26b. This vector construction adds an eight-residue tag including six C-terminal histidine residues (LEHHHHHH).

The resulting plasmids were transformed into BL21 (DE3) *Escherichia coli* competent cells. Expression was induced by treating the bacteria with 0.5 m*M* isopropyl *β*-D-thiogalactopyranoside (IPTG) overnight at 293 K. The cells expressing PIDD DD were pelleted by centrifugation, resuspended and lysed by sonication in 50 ml lysis buffer (20 m*M* Tris pH 7.9, 500 m*M* NaCl and 5 m*M* imidazole). The lysate was then centrifuged at 16 000 rev min^{-1} for 1 h at 277 K. The supernatant fractions were applied onto a gravity-flow column (Bio-Rad) packed with Ni–NTA affinity resin (Qiagen). The unbound bacterial proteins were removed from the column using wash buffer (20 m*M* Tris pH 7.9, 500 m*M* NaCl, 60 m*M* imidazole and 10% glycerol). The C-terminally His-tagged PIDD DD was eluted from the column using elution buffer (20 m*M* Tris buffer pH 7.9, 500 m*M* NaCl and 250 m*M* imidazole). 1 ml elution fractions were collected over a total of 20 ml. Fractions containing more than 80% homogeneous PIDD DD, as shown by SDS–PAGE, were selected and combined. The quantified PIDD DD and RAIDD DD proteins were mixed, with a molar excess of RAIDD DD. After pre-incubation at room temperature for 1 h, the solution was concentrated to 20–25 mg ml^{-1} using a concentration kit (Millipore). The concentrated protein complex was then applied onto a Superdex 200 gel-filtration column 10/30 (Pharmacia), which was pre-equilibrated with a solution of 20 m*M* Tris pH 8.0 and 50 m*M* NaCl. The complex elutes at around 12 ml (Fig. 1) and was collected and concentrated to 10–12 mg ml^{-1}. The complex peak was then confirmed to contain both RAIDD DD and PIDD DD by SDS–PAGE (Fig. 1).

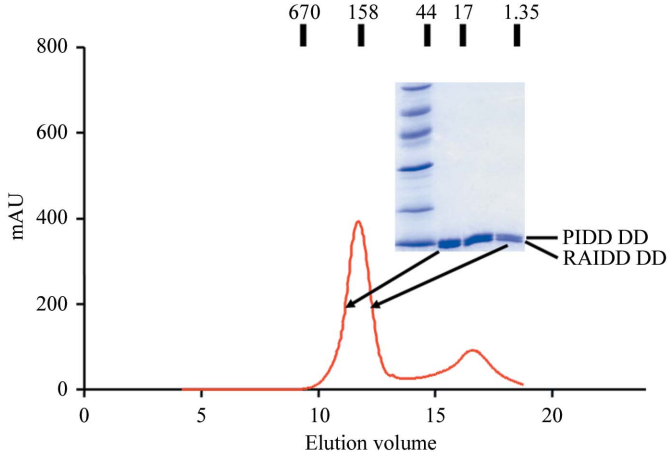

Figure 1
Gel-filtration chromatography and SDS–PAGE of the PIDD DD–RAIDD DD complex.

2.2. MALS

The absolute molecular mass of the complex was measured by static multi-angle light scattering (MALS). The pre-incubated complex was injected onto a Superdex 200 HR 10/30 gel-filtration column (Pharmacia) equilibrated with a buffer containing 20 m*M* Tris pH 8.0 and 50 m*M* NaCl. The purification system was coupled to a three-angle light-scattering detector (mini-DAWN EOS) and a refractive-index detector (Optilab DSP; Wyatt Technology). The data obtained were analyzed using the program *ASTRA*, yielding the molar mass and mass distribution (polydispersity) of the sample.

2.3. Crystallization and data collection

Crystallization conditions were initially screened at 293 K by the hanging-drop vapor-diffusion method using screening kits from Hampton Research (Crystal Screens I and II, Natrix, MembFac, SaltRX) and from deCODE Biostructures Group (Wizard I and II). Initial crystals were grown on a siliconized cover slip by equilibrating a mixture containing 1 µl protein solution (10–12 mg ml^{-1} protein in 20 m*M* Tris pH 8.0, 150 m*M* NaCl) and 1 µl reservoir solution (8% PEG 8000 in MES buffer pH 6.5) against 0.5 ml reservoir solution. The crystals were rod-shaped and only diffracted to 7–10 Å resolution.

Hexagonal shaped crystals were grown at 293 K by mixing 1 µl of the assembled complex in 20 m*M* Tris pH 8.0, 50 m*M* NaCl with 1 µl reservoir solution containing 5.5% PEG 3350, 100 m*M* sodium/potassium phosphate pH 6.5 and 200 m*M* NaCl. Crystals appeared in two weeks and grew to maximum dimensions of 0.2 × 0.2 × 0.1 mm (Fig. 2). Hg-derivative crystals were prepared by soaking in a solution containing 5.5% PEG 3350, 100 m*M* sodium/potassium phosphate pH 6.5, 200 m*M* NaCl and 1 m*M* 1,4-diacetoxymercuri-2,3-dimethoxybutane for 30 min.

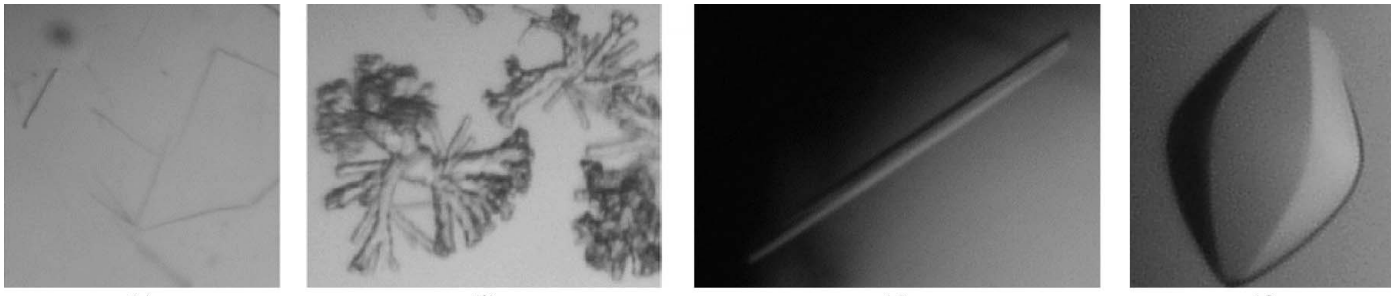

Figure 2
Crystals of the PIDD DD–RAIDD DD complex. (*a*) and (*b*) Examples of the initial crystals from different PIDD DD and RAIDD DD constructs. (*c*) A rod-shaped crystal from the best pair of PIDD DD and RAIDD DD constructs, which diffracted poorly. (*d*) A final hexagonal-shaped crystal grown in two weeks using 5.5% PEG 3350, 100 m*M* sodium/potassium phosphate and 200 m*M* NaCl. Its approximate dimensions are 0.2 × 0.2 × 0.1 mm.

For data collection, the crystals were briefly soaked in a solution corresponding to the reservoir solution supplemented with 25%(*v*/*v*) ethylene glycol. The soaked crystals were then frozen in liquid nitrogen. A 3.2 Å native diffraction data set was collected at beamline NE-CAT (24ID) of the Advanced Photon Source (APS) at Argonne National Laboratory (Fig. 3) and a 4.0 Å Hg-derivative data set was collected at beamline X4A of the National Synchrotron Light Source (NSLS) at Brookhaven National Laboratory. The data sets were indexed and processed using *HKL*-2000 (Otwinowski & Minor, 1997). Diffraction data statistics for a native and a Hg-derivative crystal are given in Table 1.

Table 1
Diffraction data statistics of PIDD DD–RAIDD DD complex crystals.

Values in parentheses are for the last resolution shell.

	Native	Hg SAD
X-ray source	NE-CAT (24ID) at APS	X4A at NSLS
Wavelength (Å)	1.0080	1.0079
Space group	$P6_5$	$P6_5$
Unit-cell parameters (Å)	$a = b = 138.4$, $c = 207.6$	$a = b = 138.9$, $c = 208.3$
Resolution limits (Å)	30–3.2 (3.31–3.20)	30–4.0 (4.14–4.00)
Mosaicity	0.67	0.6
No. of observations	374672	216211
No. of unique reflections	36257	38195
Mean $I/\sigma(I)$	40.5 (2.1)	29.7 (3.2)
Completeness (%)	97.7 (79.4)	100 (100)
R_{sym}	0.074 (0.36)	0.075 (0.42)

3. Results and discussion

Although PIDD DD and RAIDD DD are both monomeric in solution, when they were mixed together a complex containing both DDs eluted at around 150 kDa from a Superdex 200 gel-filtration column (Fig. 1). No contaminating bands are visible on SDS–PAGE of the complex. Assuming that the complex bands contain ∼10 µg protein and that the detection limit of SDS–PAGE is 0.1 µg, the purity of the complex is more than 99%. Multi-angle light scattering (MALS) with refractive-index detection, which accurately measures molecular mass regardless of shape, gave a molecular weight of the complex of 152.4 kDa with 0.8% fitting error and a polydispersity of 1.001. These data showed that PIDD DD and RAIDD DD assemble into an oligomeric complex. When the structure of the PIDD DD–RAIDD DD complex was determined, it was found that there are five molecules of PIDD DD and seven molecules of RAIDD DD in the complex (Park, Logette *et al.*, 2007). As the calculated molecular weights of monomeric PIDD DD and RAIDD DD are 13 036 and 13 075 Da, respectively, the calculated molecular weight of a 5:7 PIDD DD–RAIDD DD complex is 156.7 kDa, which agrees well with the molecular weight measured by MALS.

The success in crystallizing the PIDD DD–RAIDD DD complex is the result of several efforts. Firstly, many different PIDD DD and RAIDD DD constructs were tried, most of which either led to no crystals or poor crystals that we were not able to optimize (Figs. 2*a* and 2*b*). The best pair of PIDD DD and RAIDD DD constructs reported here initially gave rod-shaped crystals that diffracted poorly (Fig. 2*c*). Re-screening of crystallization conditions finally led to crystals of the PIDD DD–RAIDD DD complex that were hexagonal in shape (Fig. 2*d*). While most of these crystals diffracted to about 7 Å resolution, optimization of crystal handling, cryoprotection and cross-linking through screening many crystals gave diffraction to 3.2 Å resolution for a native crystal (Fig. 3) and to 4.0 Å resolution for a Hg-derivative crystal. The native crystal, data from which were collected at beamline NE-CAT (24ID), APS, belongs to space group $P6_1$ or $P6_5$, with unit-cell parameters $a = b = 138.4$, $c = 207.6$ Å. The Hg-derivative crystals were prepared by soaking the crystals in a solution containing 5.5% PEG 3350, 100 m*M* sodium/potassium phosphate pH 6.5, 200 m*M* NaCl and 1 m*M* 1,4-diacetoxymercuri-2,3-dimethoxybutane for 30 min. A single-wavelength anomalous diffraction (SAD) data set was collected from a Hg-derivative crystal at beamline X4A, NSLS.

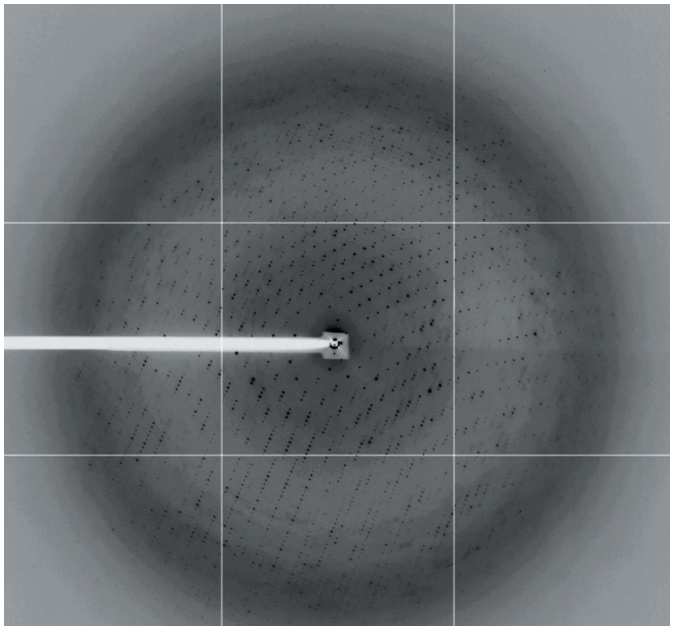

Figure 3
A diffraction image (1° oscillation) of the PIDD DD–RAIDD DD native crystal with 3.2 Å resolution limit.

The structure of the PIDD DD–RAIDD DD complex was determined by SAD phasing using the Hg-derivative data set at 4.0 Å resolution (Park, Logette *et al.*, 2007). There is a single partially surface-exposed free cysteine in RAIDD DD (Park & Wu, 2006) and there are no cysteines in PIDD DD. Five Hg sites were found using the program *SOLVE* and phase determination identified the hand of the space group to be $P6_5$ (Terwilliger & Berendzen, 1997). A six-dimensional phased translation-function search of the electron density using the RAIDD DD structure found ten DD molecules in the crystallographic asymmetric unit, five of which correspond to PIDD DD. Although RAIDD DD and PIDD DD share a limited sequence identity of ∼14%, they have the same six-helical bundle fold characteristic of death domains. After several refinement steps using *CNS* (Brünger *et al.*, 1998), two more RAIDD DD molecules were found, giving a total of seven RAIDD DD and five PIDD DD molecules in the asymmetric unit. The Matthews coefficient (V_M) was calculated to be 3.65 Å^3 Da^{-1}, which corresponds to a solvent content of 66.3% (Matthews, 1968). The initial model was modified and built into the electron-density map using *O* (Jones *et al.*, 1991). The structure has been refined and described elsewhere (Park, Logette *et al.*, 2007).

We thank Upendra Maddineni for proofreading the manuscript. We are grateful to Drs Kanagalaghatta Rajashankar and Igor Kourinov at NE-CAT (24ID) of the Advanced Photon Source and Drs John Schwanof and Randy Abramowitz at X4A of the National Synchrotron Light Source for help with data collection. We also

thank Dr Jin Wu for maintaining our X-ray facility and computing resources.

References

Brünger, A. T., Adams, P. D., Clore, G. M., DeLano, W. L., Gros, P., Grosse-Kunstleve, R. W., Jiang, J.-S., Kuszewski, J., Nilges, M., Pannu, N. S., Read, R. J., Rice, L. M., Simonson, T. & Warren, G. L. (1998). *Acta Cryst.* D**54**, 905–921.
Jones, T. A., Zou, J.-Y., Cowan, S. W. & Kjeldgaard, M. (1991). *Acta Cryst.* A**47**, 110–119.
Lassus, P., Opitz-Araya, X. & Lazebnik, Y. (2002). *Science*, **297**, 1352–1354.
Martinon, F., Burns, K. & Tschopp, J. (2002). *Mol. Cell*, **10**, 417–426.
Matthews, B. W. (1968). *J. Mol. Biol.* **33**, 491–497.
Otwinowski, Z. & Minor, W.(1997). *Methods Enzymol.* **276**, 307–326.
Park, H. H., Lo, Y., Lin, S., Wang, L., Yang, J. K. & Wu, H. (2007). *Annu. Rev. Immunol.* **25**, 561–586.
Park, H. H., Logette, E., Raunser, S., Cuenin, S., Walz, T., Tschopp, J. & Wu, H. (2007). *Cell*, **128**, 533–546.
Park, H. H. & Wu, H. (2006). *J. Mol. Biol.* **357**, 358–364.
Reed, J. C., Doctor, K. S. & Godzik, A. (2004). *Sci. STKE*, re9.
Riedl, S. J. & Shi, Y. (2004). *Nature Rev. Mol. Cell Biol.* **5**, 897–907.
Tinel, A. & Tschopp, J. (2004). *Science*, **304**, 843–846.
Salvesen, G. S. & Dixit, V. M. (1999). *Proc. Natl Acad. Sci. USA*, **96**, 10964–10967.
Terwilliger, T. C. & Berendzen, J. (1997). *Acta Cryst.* D**53**, 571–579.
Wajant, H. (2002). *Science*, **296**, 1635–1636.
Zou, H., Hemel, W. J., Liu, X., Lutsch, A. & Wang, X. (1997). *Cell*, **90**, 389–390.